agriculture

MDPI

Article

Design and Experimentation of Targeted Deep Fertilization Device for Corn Cultivation

Zhongying Qi, Cunliang Liu, Yao Wang, Zhiwei Zhang and Xiaobo Sun *

College of Engineering, Northeast Agricultural University, Harbin 150030, China; qzy@neau.edu.cn (Z.Q.); s220702020@neau.edu.cn (C.L.); s220702001@neau.edu.cn (Y.W.); s230702041@neau.edu.cn (Z.Z.)
* Correspondence: sunxiaobo@neau.edu.cn; Tel.: +86-132-6350-6609

Abstract: In response to the challenges of low fertilizer utilization rates, excessive application amounts, and difficulties in precise targeted fertilization during the middle tillage and top-dressing period for corn, a targeted deep fertilization device is designed, integrating mechanical structure design and automatic control technology. The device mainly includes a strong discharge fertilization device and a targeted fertilization control system. The fertilization device has been designed, and the main factors affecting the performance of the fertilization wheel have been identified. Based on the structure, a strong discharge fertilization plate mechanism has been added, and a mechanical model for the fertilization wheel during the refilling and discharging processes has been constructed. A targeted fertilization control system for corn has been developed that utilizes a photoelectric sensor to detect the position of the corn plants. A microcontroller combines the plant position information and the device moving speed to adjust the intermittent rotation of the stepper motor in real time, achieving targeted deep fertilization for corn. Coupled simulation analysis was conducted using discrete element software EDEM and dynamic software Adams. Through single-factor and multi-factor experiments, the main factors affecting fertilization performance were analyzed, and the optimal structural parameters for the fertilization wheel were determined. Bench validation tests were conducted, and the results demonstrated that under forward speeds of 0.4 to 1.2 m/s, the coefficient of variation of the fertilizer application rate per hole of the discharge device ranged from 2.02% to 4.46%, the error in fertilizer application rate per hole ranged from 7.12% to 12.18%, the average length of fertilizer application holes ranged from 72.5 mm to 130.2 mm, and the coefficient of variation of hole length stability ranged from 1.94% to 3.54%. These parameters were consistent with the results from the simulation tests, and the operational performance met the requirements. Finally, field tests validated the overall operational performance of the device. When the device's speed ranged from 0.4 m/s to 1.2 m/s, the coefficient of variation of the fertilizer application rate per hole, the error in fertilizer application rate per hole, the average length of fertilizer application holes, the coefficient of variation of hole length stability, and the qualification rate of fertilization position were 3.63%, 10.46%, 108.8 mm, 2.96%, and 87.16%, respectively. The overall performance of the device is stable and meets the requirements for targeted deep fertilization in corn cultivation.

Keywords: targeted deep fertilization; fertilizer discharge device; coupled simulation analysis; photoelectric sensor

Citation: Qi, Z.; Liu, C.; Wang, Y.; Zhang, Z.; Sun, X. Design and Experimentation of Targeted Deep Fertilization Device for Corn Cultivation. *Agriculture* **2024**, *14*, 1645. https://doi.org/10.3390/agriculture14091645

Academic Editor: Takashi Okayasu

Received: 31 August 2024
Revised: 15 September 2024
Accepted: 18 September 2024
Published: 20 September 2024

1. Introduction

Corn is one of the major crops in China, playing a vital role in ensuring food security and economic development [1]. However, during production, the blind over-application of chemical fertilizers has caused a series of issues, including food safety concerns, environmental pollution, and resource waste [2]. Targeted fertilization technology allows for precise and quantitative fertilization of corn at the seedling stage, achieving the goals of reducing fertilizer usage while enhancing quality and scientific application [3], thereby aligning with China's agricultural sustainable development strategy.

To improve fertilization accuracy and the precision of application positions, Chinese scholars have primarily focused on developing automatic control systems for variable fertilizer application and creating hole-application fertilization equipment. For instance, Hu Hong et al. designed a point-based deep fertilization machine for corn [4], which locates the fertilization position using plant position detection mechanisms and a ratchet clutch mechanism. Li et al. implemented a mechanical touch identification device combined with a crank-rocker mechanism for precise hole-style fertilization of inter-row crops [5]. Wang et al. developed a roller-type corn hole applicator with six flat-nose hole makers [6]; it increases fertilization position accuracy by designing the fixed wheel circumference in relation to the spacing between plants. Wang et al. built an experimental platform for variable hole fertilization in corn [7], controlling the precise start-stop operation of a stepper motor and designing a baffle for the fertilizer discharge outlet to achieve targeted fertilization. Zhao et al. designed a motor-driven positioning fertilization control system that collects real-time ground speed and fertilization position information to achieve precise point application of fertilizers [8].

In the aforementioned study, a mechanical structure was developed to achieve targeted fertilization during the seedling stage of corn, enabling precise fertilization of cultivated crops. However, the complexity of the structure, along with the susceptibility of positioning accuracy to environmental conditions, poses challenges in ensuring effective fertilizer placement in holes. Although fertilizing machines based on positioning control systems can achieve accurate positioning, their control systems are complicated and have limited applicability [9]. Considering the limited research on targeted fertilization tools for corn during the tillage period, as well as issues related to structural complexity and poor performance in creating fertilizer placement holes, a targeted deep fertilization device for corn has been designed by integrating mechanical structure and automatic control technology. A fertilizer distribution device featuring a distribution board mechanism was designed. Through theoretical analysis and simulation tests, the key structures of the fertilizer distribution device were identified, significantly improving the effectiveness of fertilizer placement. Bench tests were also conducted to validate the rationality of the simulation tests. Furthermore, utilizing the synergistic effect of photoelectric sensors and stepper motors, a control system for targeted fertilization in corn was developed. Finally, field experiments were carried out to verify the operational performance of the overall system.

2. Materials and Methods

2.1. Overall Structure of Targeted Deep Fertilization Device for Corn

The targeted deep fertilization device for corn primarily consists of a frame, trenching tool, ground wheel, fertilization device, fertilizer tube, and targeted fertilization control system. The trenching tool, ground wheel, fertilization device, and targeted fertilization control system are all mounted on the frame, and the fertilizer tube connects the discharge outlet of the fertilization device to the drop outlet of the trenching tool. The fertilization device mainly comprises a fertilizer box, stepper motor, coupling, drive shaft, and discharge device. The targeted fertilization control system consists primarily of a photoelectric sensor, stepper motor, and control box. The overall structure of the device is illustrated in Figure 1.

2.2. Working Principle

The targeted deep fertilization device for corn connects to the tractor via a three-point hitch mounted on the frame. During field operation, the trenching tool enters the soil first. When the photoelectric sensor is obstructed by a plant in the direction of travel, it detects a signal and transmits it to the control box. This action controls the rotation of the stepper motor, which drives the discharge device to release the fertilizer. The discharged fertilizer then travels through the fertilizer tube and falls into the furrow created by the trenching tool. The operational effect of the device is illustrated in Figure 2.

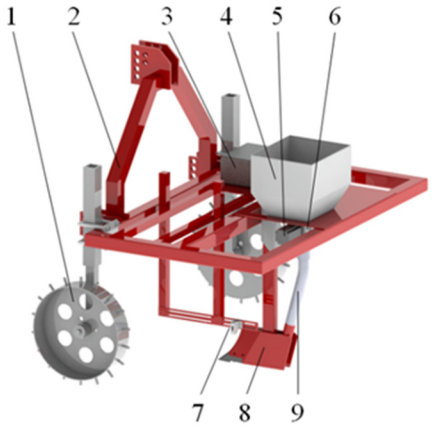

Figure 1. Structure diagram of maize targeted deep fertilization device. 1. Ground wheel. 2. Machine frame. 3. Control box. 4. Fertilizer tank. 5. Stepper motor. 6. Fertilizer distribution system. 7. Photoelectric sensor. 8. Ditch digger. 9. Fertilizer pipe.

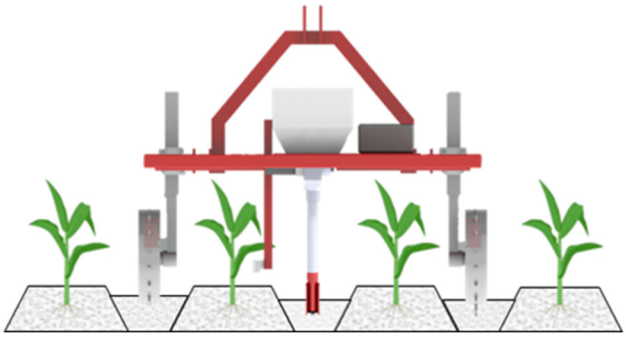

Figure 2. Operation diagram of maize targeted deep fertilization device.

Interventional studies involving animals or humans, and other studies that require ethical approval, must list the authority that provided approval and the corresponding ethical approval code.

2.3. Structure Design and Analysis of Fertilizer Discharge Device

2.3.1. Structure and Working Principle

The discharge device mainly consists of components such as a shell, brushes, discharge wheels, and fertilizer protection belts [10]. It is divided into four working areas sequentially: I. Fertilizer Filling Area, II. Fertilizer Protection Area, III. Fertilizer Discharge Area, and IV. Transition Area. The structure of the discharge device is illustrated in Figure 3.

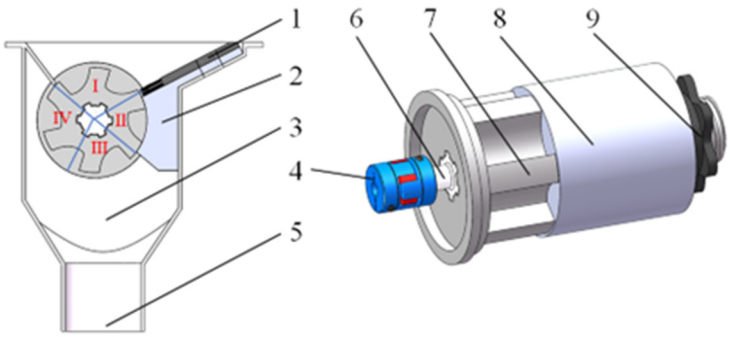

(**a**) Division of work areas. (**b**) Fertilizer discharge mechanism.

Figure 3. Structure diagram of fertilizer discharge device. 1. Brush. 2. Fertilizer guard belt. 3. Housing. 4. Coupling. 5. Fertilizer outlet. 6. Drive shaft. 7. Fertilizer spreader wheel. 8. Block wheel. 9. Fertilizer flow adjustment knob.

During operation, the stepper motor drives the output shaft to rotate through a coupling, causing the discharge wheel and the fertilizer quantity adjustment knob to rotate synchronously. As the discharge wheel moves from the transition area to the fertilizer filling area, fertilizer particles begin to fill into the discharge trough. As the discharge wheel continues to rotate, excess fertilizer is brushed off by the brushes as it passes into the fertilizer protection area, where the protection belt ensures that the fertilizer remains intact and does not break. Finally, the wheel moves to the discharge area, where the fertilizer exits through the discharge opening.

The amount of fertilizer applied can be adjusted by the fertilizer quantity adjustment knob, which changes the relative overlapping length between the discharge wheel and the blocking wheel in the discharge trough. This mechanism allows for precise control over the fertilization rate.

2.3.2. Structural Parameter Analysis

This study is designed based on the common groove wheel used in standardized production. After practical measurement, the parameters are as follows: the diameter (D) of the fertilizer distribution wheel is 63 mm, the number of grooves on the distribution wheel is 6, and the maximum effective working length of the distribution wheel is 60 mm.

The shape of the discharge trough impacts the volume of fertilizer as well as the filling and discharging processes [11]. During the filling phase, fertilizer particles initially slide in along the right wall of the discharge trough. During the discharging phase, the particles slide out along the same wall. To meet the design requirements for easier filling and discharging of fertilizer particles, a smooth curve is introduced along the left wall of the discharge trough. This curve is tangent to the right wall and represents half of a cycloidal arc. Its structure is illustrated in Figure 4.

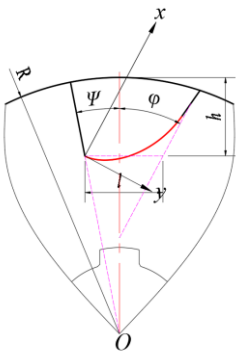

Figure 4. Structure diagram of fertilizer drainage tank.

The parametric equations of the cycloid are as follows:

$$\begin{cases} x = a(\theta - \sin\theta) \\ y = a(1 - \cos\theta) \\ a = (R - h)\tan\psi\cos\varphi \\ \tan\psi = \frac{l}{2(R-h)} \end{cases} \quad (1)$$

where x is the x-coordinate of the cycloid, mm; where y is the y-coordinate of the cycloid, mm; where a is cycloidal parameters, mm; where θ is parameters of the cycloid, rad; where h is the depth of the fertilizer channel, mm; where R is the radius of the fertilizer distribution wheel, mm; where l is the bottom width of the fertilizer channel, mm; where Ψ is the left wall inclination of the fertilizer channel; and where φ is the right wall inclination of the fertilizer channel.

From Equation (1), it can be seen that under the condition of a fixed radius for the fertilizer distribution wheel, the equation of the cycloid is determined by the depth of

the fertilizer channel, the left wall inclination of the fertilizer channel, and the right wall inclination of the fertilizer channel.

In Northeast China, the recommended urea fertilizer application for spring corn is between 245 and 326 kg/hm² [12]. Targeted fertilization can improve fertilizer utilization and reduce the amount applied. Therefore, when setting the fertilization amount, the lower limit should be appropriately adjusted, establishing a range of 190 to 326 kg/hm². The row and plant spacing for corn is 60 cm × 33 cm, resulting in a single corn plant receiving a fertilization amount of 3.8 to 6.5 g.

The fertilization amount per corn plant depends on the volume of the fertilizer slot, and the volume calculation formula is as follows:

$$\begin{cases} V_0 = S_0 l_0 \\ S_0 = \frac{\pi\psi R^2}{360} - \frac{l(R-h)}{4} + \frac{\pi\varphi\left(h+\frac{l}{2\tan\varphi}\right)^2}{360} \\ -\frac{l^2}{8\tan\varphi} + al\sin\varphi - \frac{\pi a^2}{2} \end{cases} \quad (2)$$

where V_0 is the volume of the fertilizer channel, mm^3; where S_0 is the cross-sectional area of the fertilizer channel, mm^2; and where l_0 is the working length of the fertilizer distribution groove, mm.

According to the requirements for the fertilization amount per corn plant, the design parameters for the fertilizer slot are as follows: the left wall inclination of the fertilizer slot is set at 15°, the right wall inclination is in the range of 32° to 44°, the depth of the fertilizer slot ranges from 7 to 15 mm, and the working length of the fertilizer slot ranges from 30 to 58 mm.

Since an intermittent fertilizer distribution method is used, with the distance (S) between the position of the photoelectric sensor and the fertilizer dropping outlet, when the machine advances a distance (S), the fertilizer distribution wheel rotates once, with each rotation covering 60°. Therefore, the linear speed of the fertilizer distribution wheel is as follows [13]:

$$v_p = \frac{2\pi R v_m}{SZ} \quad (3)$$

where v_p is the linear velocity of the fertilizer distribution wheel, m/s; where v_m is the forward speed of the machinery, m/s; where Z is the number of fertilizer distribution grooves, 6; and where S is the set to install as 150 mm.

Therefore, when the machine's forward speed is between 0.4 and 1.2 m/s, the corresponding rotation speed of the fertilizer distribution wheel is between 26.67 and 80 r/min.

2.3.3. Structure Design and Working Principle of Strong Discharge Fertilizer Distribution Board

Based on the structure of the fertilizer channel, the left wall of the fertilizer channel is designed to be a swingable structure. When the fertilizer distribution wheel moves from the fertilizer protection area to the fertilizer distribution area, the fertilizer plate will rotate, allowing the fertilizer inside the fertilizer slot to be quickly discharged [14]. The structure of the fertilizer plate is shown in Figure 5.

Fertilizer plate (a) is mounted at one end on the end face of the fertilizer distribution wheel through a spring plunger, allowing the swinging plate to rotate around the spring plunger. The other end of fertilizer plate (a) is nested inside fertilizer plate (b). The other end of fertilizer plate (b) is connected to the end face of the blocking wheel via a spring plunger and can also rotate around it. When the fertilizer slot is about to turn toward the fertilizer distribution area, fertilizer plate (a) is blocked by a fixed bolt installed on the motor fixture, which drives fertilizer plate (b) to rotate along with it, quickly discharging the fertilizer. Subsequently, under the action of the reset spring, both fertilizer plates (a) and (b) return to their original positions, completing one quick fertilizer discharge cycle.

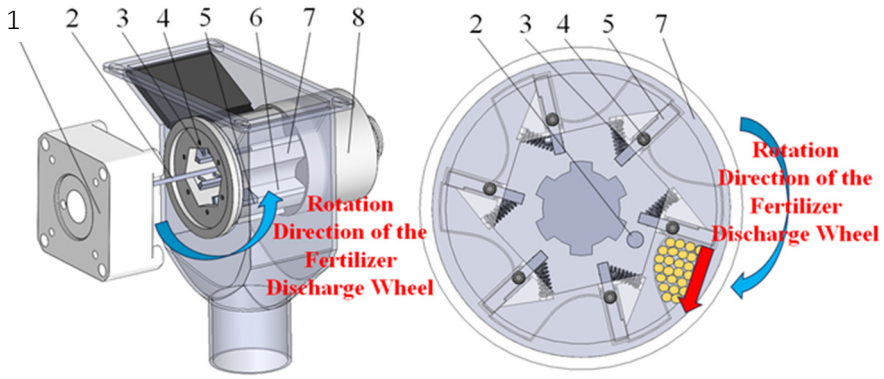

(**a**) (**b**)

Figure 5. Fertilizer board structure diagram. 1. Motor fixture. 2. Fixed bolt. 3. Reset spring. 4. Spring plunger. 5. Fertilizer plate. (**a**) 6. Fertilizer plate. (**b**) 7. Fertilizer distribution wheel. 8. Blocking wheel.

2.3.4. Mechanical Analysis of the Fertilizer Filling Process

When the fertilizer distribution wheel rotates to the filling area, the fertilizer particles first enter the fertilizer channel along the right wall of the channel. The time required for the fertilizer particles to fill the channel is a key factor influencing filling performance. An analysis of the filling process focuses on a single fertilizer particle [15]. In the initial stage of filling, since the fertilizer has not yet completely filled the channel, the pressure exerted on the fertilizer particle is equal to the total mass of the fertilizer particles above it, while neglecting the lateral pressure. Taking the centroid of the fertilizer particle as the origin of the coordinate system, we establish the coordinate system shown in Figure 6. The x-axis passes through the center (O) of the fertilizer distribution wheel and points toward the outside of the wheel from the centroid (P) of the fertilizer particle, while the y-axis is perpendicular to the x-axis and points in the direction of the wheel's rotation [16].

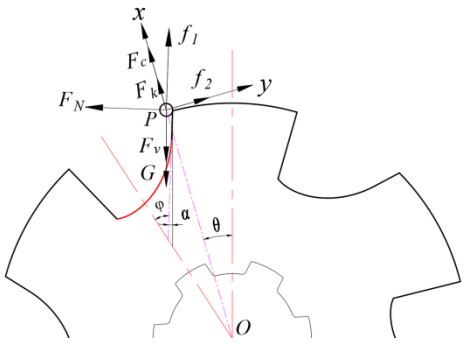

Figure 6. Force analysis of fertilizer filling link.

Fertilizer particles fill the slot under the influence of their own weight (G), the pressure from the upper layer of fertilizer particles, centrifugal force, Coriolis force during motion, the support force from the right wall of the fertilizer channel, the frictional force from the right wall of the fertilizer channel on the fertilizer particles, and the frictional force between the fertilizer particles. The mechanical equilibrium equation in the filled state is as follows:

$$\begin{cases} ma_n = F_v + G + F_N \sin\alpha - (F_c + F_k)\cos\theta - f_1 \cos\alpha \\ ma_\tau = F_N \cos\alpha + (F_c + F_k)\sin\theta + f_1 \sin\alpha - f_2 \\ F_c = mr{\omega_r}^2 \\ F_k = 2m\omega v_r \\ f_1 = \mu_1 F_N \\ f_2 = \mu_2 F_v \\ G = mg \end{cases} \quad (4)$$

where m is the quality of fertilizer granules, kg; where a_n is the normal acceleration of fertilizer particles, m/s^2; where a_τ is the tangential acceleration of fertilizer particles, m/s^2; where α is the angle between the right wall of the fertilizer distribution channel and the vertical direction, °; where θ is the fertilizer filling angle, which is the angle between OP and the vertical direction, °; where r is the distance from the centroid P of the fertilizer particle to the center O of the fertilizer distribution wheel, m; where ω_r is the relative angular velocity between the fertilizer particle and the fertilizer distribution wheel, rad/s; where ω is the angular velocity of the fertilizer distribution wheel, rad/s; where v_r is the relative velocity between the fertilizer particles and the fertilizer distribution wheel, m/s; where μ_1 is the friction coefficient between the fertilizer and the right wall of the fertilizer distribution chute; and where μ_2 is the friction coefficient between fertilizer particles.

Further derivation yields the calculation formulas for the normal acceleration (a_n), tangential acceleration (a_τ), and the displacement (H) in the normal direction along the cross-section of the fertilizer distribution wheel for the relative motion of fertilizer particles:

$$\begin{cases} a_n = \frac{1}{m}[F_v + G + F_N \sin\alpha - (F_c + F_k)\cos\theta - f_1 \cos\alpha] \\ a_\tau = \frac{1}{m}[F_N \cos\alpha + (F_c + F_k)\sin\theta + f_1 \sin\alpha - f_2] \\ H = \frac{1}{2} a_n t^2 \end{cases} \tag{5}$$

where t is the time taken for fertilizer particles to slide into the bottom of the fertilizer distribution chute, s.

Further derivation leads to the following:

$$t = \sqrt{\frac{2hm}{F_v + G + F_N \sin\alpha - (F_c + F_k)\cos\theta - f_1 \cos\alpha}} \tag{6}$$

Based on Equation (6), it can be concluded that when the fertilization angle (θ) is fixed, reducing the displacement (H) of fertilizer particles in the normal direction along the cross-section of the fertilizer distribution wheel and increasing the angle (α) between the right wall of the fertilizer outlet and the vertical direction can effectively reduce the time taken for fertilizer particles to enter the outlet. Therefore, it is advisable to appropriately reduce the depth (h) of the fertilizer outlet and increase the inclination angle (φ) of the right wall of the fertilizer outlet. Further analysis will continue on the depth (h) of the fertilizer outlet and the inclination angle (φ) of the right wall.

2.3.5. Mechanical Analysis of the Fertilizer Discharge Process

When the fertilizer distribution wheel rotates to the distribution zone, the fertilizer particles are ejected from the outlet under the influence of centrifugal force, gravity, and the force exerted by the distribution plate. The velocity of the fertilizer particles at the moment they are ejected by the distribution plate significantly affects the cavity formation on the ground after the fertilizer falls. Therefore, an analysis of the motion of the fertilizer expelled by the distribution plate is conducted, treating a single fertilizer particle as the subject of study. After leaving the outlet, the fertilizer performs a projectile motion at an angle, as shown in Figure 7.

The initial velocity is the sum of the tangential velocities at the outer edge of the fertilizer discharge wheel and the tangential velocity at the outer edge of the fertilizer discharge plate, denoted as (v_0). It can be decomposed into horizontal velocity (v_x) and vertical velocity (v_y), with the components in each direction being as follows:

$$\begin{cases} v_0 = \omega R + \omega_b l \\ v_x = v\cos\beta \\ v_y = v\sin\beta \\ \omega_b = 1.68\omega \end{cases} \tag{7}$$

where ω is the angular velocity of the fertilizer discharge wheel, rad/s; where R is the radius of the fertilizer discharge wheel, m; where ω_b is the angular velocity of the fertilizer discharge plate, rad/s; and where l is the depth of the fertilizer channel, m.

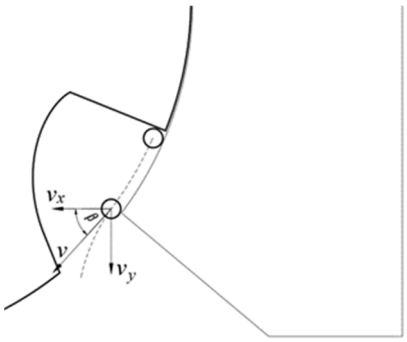

Figure 7. Force analysis of fertilizer filling link.

The displacement of the fertilizer is represented by Z, which can be decomposed into the horizontal displacement x and the vertical displacement y, as follows:

$$\begin{cases} Z = \sqrt{x^2 + y^2} \\ x = v_x t \\ y = v_y t + \frac{1}{2} g t^2 \end{cases} \quad (8)$$

According to Equations (7) and (8), it can be seen that the influence of the distribution plate effectively increases the velocity at which the fertilizer is discharged. With the same displacement, the time for fertilizer application is shortened, which directly affects the distribution length of the fertilizer upon landing, thereby improving the effectiveness of cavity formation.

2.4. Targeted Fertilization Control System for Corn

When the device operates in the field, the system utilizes a photoelectric sensor to detect the root-stem part of the corn plants and obtain their positional information. The microcontroller then adjusts the stepping motor's speed in real time based on the forward speed of the device, controlling the intermittent rotation of the stepping motor to achieve targeted deep fertilization for the corn [17]. The structural composition of the targeted fertilization control system is shown in Figure 8.

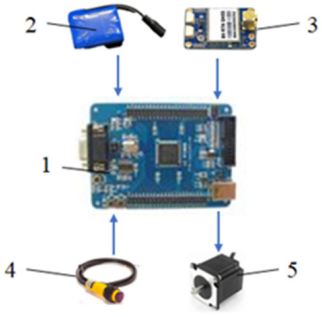

Figure 8. Structure and components of the targeted fertilization control system. 1. Microcontroller. 2. Storage battery. 3. GNSS speed measurement module. 4. Photoelectric sensor. 5. Stepper motor.

2.4.1. System Hardware

The circuit diagram of the system is shown in Figure 9.

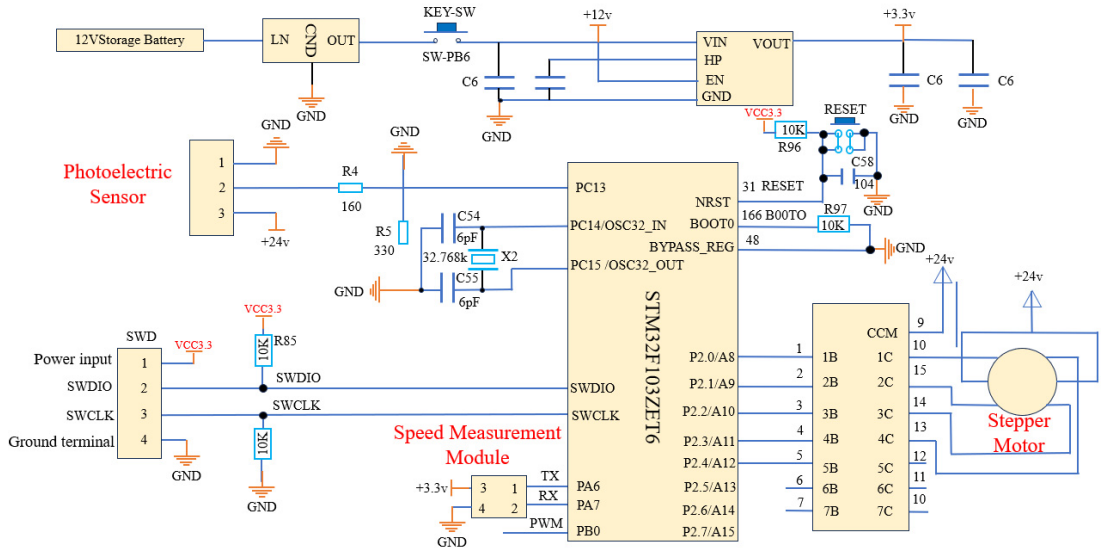

Figure 9. Targeted fertilization control system circuit.

The hardware workflow is illustrated in Figure 10. The controller uses the STM32F103ZET6 microcontroller, which has a main frequency of 72 MHz [18]. The photoelectric sensor is a CZ3460 diffuse reflection type produced by Domenzi, capable of detecting objects at a distance of 4 to 40 cm, with a working voltage of 24 V and a working current of 0.02 A; its response time is less than 2 ms [19]. The GNSS module is produced by Beitian and is an RTK-GNSS module that combines GPS and BeiDou, with a speed accuracy of 0.05 m/s [20]. The actuator is a 57–3.6 nm stepping motor produced by Luyue Technology Company, operating at a DC voltage of 24 V, with a rated current of 4 A and a step angle of 1.8°.

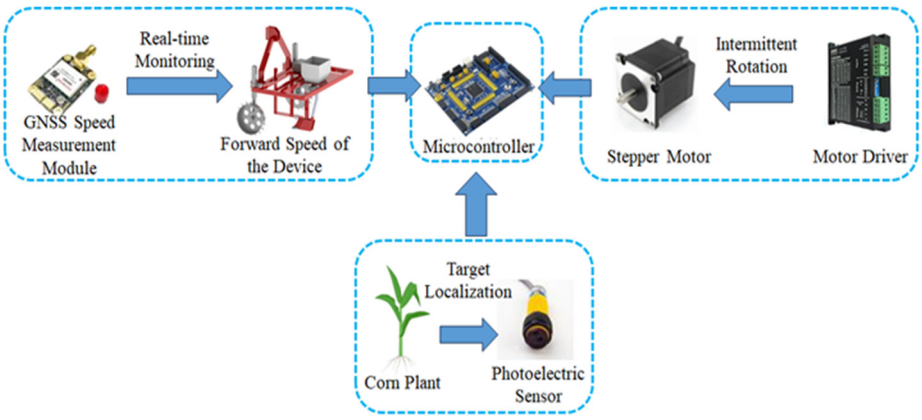

Figure 10. Schematic diagram of targeted fertilization control system hardware process.

2.4.2. System Program

The system program workflow is illustrated in Figure 11. First, the system initializes. Subsequently, the system begins operation, with the speed measurement module continuously monitoring the forward speed of the device. When the photoelectric sensor detects the positional information of the plants, the microcontroller calculates the stepping motor speed based on the operating speed of the device. The motor driver then drives the stepping motor to rotate intermittently, allowing the fertilizer dispenser to complete the discharge of fertilizer, thereby completing a targeted fertilization operation.

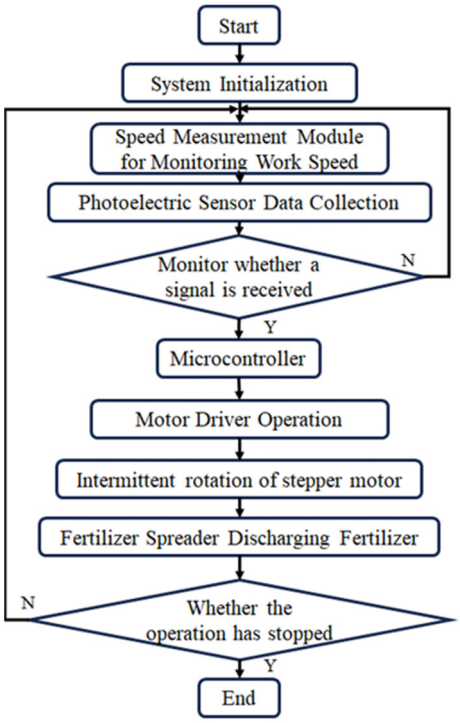

Figure 11. System program workflow.

3. Simulation Analysis of Fertilizer Discharge Device Performance

3.1. Construction of a Discrete Element Simulation Platform

Due to the passive rotation of the fertilizer distribution plate under the obstruction of fixed bolts during the fertilizer application process, a standalone simulation using EDEM software cannot accurately represent this motion. Therefore, a coupled simulation using the dynamics simulation software Adams in conjunction with EDEM is employed for the relevant analysis [21].

The model of the fertilizer distribution device, created using SolidWorks 2021, is saved in STEP format and imported into Adams 2020 to establish a dynamic model. A rotational joint is added between the fertilizer distribution plate and the shaft, and a torsional spring damper is created between the fertilizer distribution plate and the fertilizer wheel. Contact points are established between the fixed bolts and each fertilizer distribution plate. A velocity (time) type drive function is added to the fertilizer wheel, with the function expression defined as the following: if (time-1:0, 0, if (mod (time-1, 0.4)-0.2:-300d, 0, 0)). This means that the fertilizer wheel completes a periodic rotation every 0.2 s, with each rotation being 60°. Additionally, G-forces are applied to each component. The coupling interface between Adams and EDEM is established through Adams Co-simulation [22].

The STEP format file of the fertilizer distribution device is imported into EDEM 2020 to establish a discrete element model for the fertilizer distribution device and fertilizer particles, as shown in Figure 12. Since the fertilizer is classified as nearly spherical particles with a sphericity of over 90%, the simulation model can replace the fertilizer particles with spheres. The particle model is set to a diameter of 3.02 mm, and the contact model for both particle-to-particle and particle-to-geometry is selected as the Hertz–Mindlin no-slip contact model. A particle factory is added above the fertilizer box, with the initial particle velocity set to vz = −1 m/s and the gravitational acceleration set to g = 9.81 m/s². A total of 45,000 fertilizer particles are generated within 1 s. A conveyor belt is set at the bottom of the fertilizer distribution device to simulate soil, with its length calculated as the product of the travel speed and the time step, where the travel speed is 0.6 m/s. The simulation time step is set to 8 s, and data are saved every 0.01 s. Simulation parameters are shown in Table 1 [23].

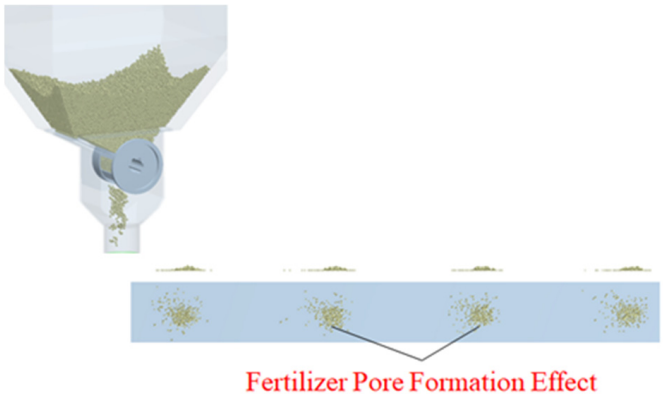

Figure 12. Simulation model.

Table 1. Simulation parameters.

Stats	Parameter	Value
Fertilizer Granules	Density/(g·cm^3)	1.575
	Shear Modulus/(GPa)	0.125
	Poisson's Ratio	0.250
PLA	Density/(g·cm^3)	1.240
	Shear Modulus/(GPa)	0.130
	Poisson's Ratio	0.430
Soil	Density/(g·cm^3)	1.357
	Shear Modulus/(GPa)	0.727
	Poisson's Ratio	0.35
Fertilizer Granules—Fertilizer Granules	Coefficient of Restitution	0.31
	Coefficient of Static Friction	0.37
	Coefficient of Rolling Friction	0.12
Fertilizer Granules—PLA	Coefficient of Restitution	0.41
	Coefficient of Static Friction	0.32
	Coefficient of Rolling Friction	0.18
Fertilizer Granules—Soil	Coefficient of Restitution	0.02
	Coefficient of Static Friction	1.25
	Coefficient of Rolling Friction	1.24

3.2. Fertilization Performance Evaluation Method

Based on the aforementioned research, the right wall angle of the fertilizer distribution trough, the depth of the trough, and the working length of the trough are selected as experimental factors, with the coefficient of variation of the fertilizer distribution amount per hole and the average hole length selected as the experimental indicators [24].

In the EDEM post-processing interface, a geometry bin is added at the middle position of the bottom plane parallel to the conveyor belt through the selection group [25]. The width of the geometry bin is consistent with that of the conveyor belt, the height is set to 20 mm, and the length is calculated as the product of the conveyor belt speed and the data-recording time interval (0.01 s) [26]. The mass of the fertilizer within the geometry bin is recorded every 0.01 s, collecting data for 10 fertilizer particles per hole each time. The coefficient of variation of the fertilizer distribution amount per hole and the average hole length are calculated, with the formulas for each experimental indicator being as follows:

$$\begin{cases} X = \dfrac{1}{n}\sum\limits_{i=1}^{n} X_i \\ C_V = \sqrt{\dfrac{1}{n-1}\sum\limits_{i=1}^{n}(X_i - X)^2} \times 100\% \\ L = \dfrac{1}{n}\sum\limits_{i=1}^{n} v_c t_i \end{cases} \tag{9}$$

where X is the average value of single fertilizer application weight, g; where n is the number of fertilizer holes; where X_i is the fertilizer granule weight per hole, g; where C_V is the coefficient of variation of the fertilizer application rate per hole, %; where L is the average length of fertilizer application holes per single application, mm; where v_c is the conveyor belt speed, m/s; and where t_i is the time for fertilizer to pass through the geometry bin per hole, s.

3.3. Design of Single-Factor Tests

In conducting experiments for a specific factor, the control variable method is used to quantitatively control the other two factors, allowing for the verification of the effect of a single factor on the experimental indicators [27]. The influence of different factors on the coefficient of variation of fertilizer distribution per hole and the average hole length is illustrated in Figure 13.

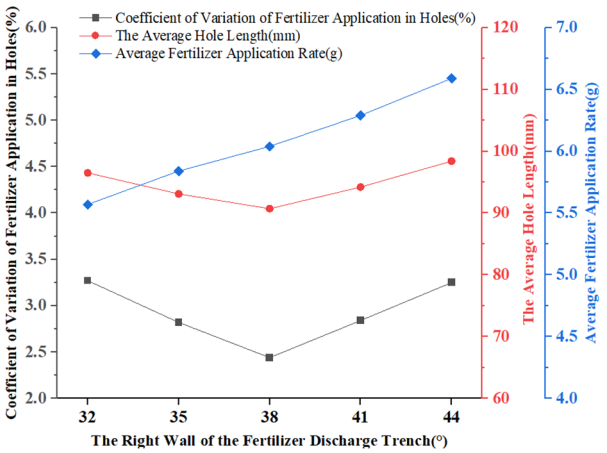

(**a**) Effect of the right wall of the fertilizer discharge trench on experimental indicators.

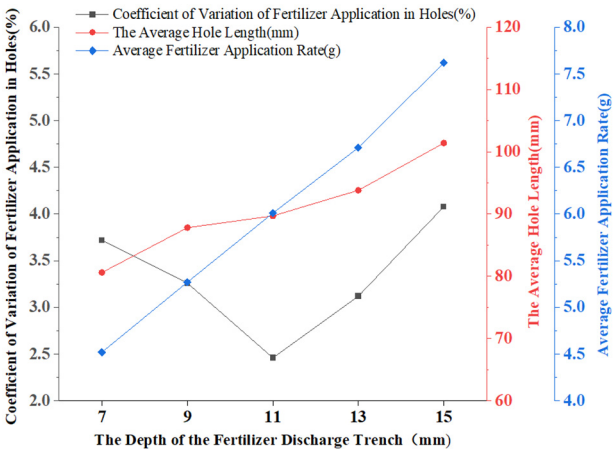

(**b**) Effect of the depth of the fertilizer discharge trench on experimental indicators.

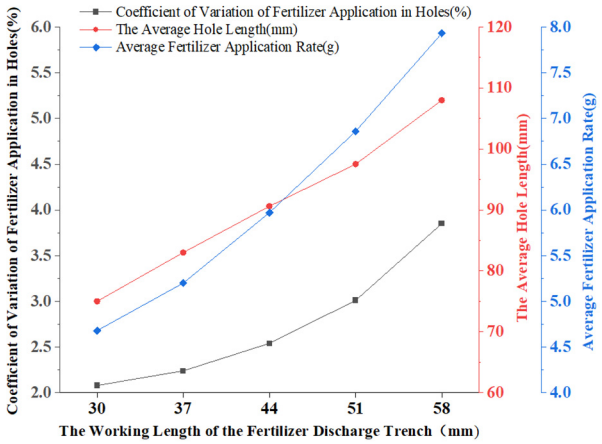

(**c**) Effect of the working length of the fertilizer discharge trench on experimental indicators.

Figure 13. Effects of various factors on experimental indicators.

As the angle of the right wall of the fertilizer distribution trough and the depth of the trough increase, the average fertilizer distribution amount gradually increases, while the coefficient of variation of the fertilizer distribution amount per hole and the average hole length also gradually increase. When the angle of the right wall and the depth of the trough are relatively small, the amount of fertilizer that can be filled decreases, making it easier for the already filled fertilizer to detach from the trough. Conversely, when the angle of the right wall and the depth of the trough are relatively large, there is an increase in the amount of fillable fertilizer, resulting in some fertilizer not completely filling the trough.

Additionally, as the working length of the fertilizer distribution trough increases, the average fertilizer distribution amount, the coefficient of variation of the fertilizer distribution amount per hole, and the average hole length all show a gradual increasing trend.

3.4. Multi-Factor Experiment

The above experimental analysis indicates that the right wall angle of the fertilization trough, the depth of the trough, and the working length of the trough are closely related to fertilization performance, with the best fertilization effect observed within this context. Based on the analysis of the single-factor experiments, the range for the right wall angle of the fertilization trough was set at 35–41°, the depth at 9–13 mm, and the working length at 30–44 mm. Using the variation coefficient of the fertilization amount in the holes and the average hole length as experimental indicators, a three-factor, three-level quadratic regression orthogonal experiment was designed to optimize the structural parameters of the fertilization wheel and determine the best combination [28]. The experimental factors and levels are shown in Table 2. The experimental scheme and results are presented in Table 3. Experiments on a total of 17 experimental groups were conducted, with each group repeated three times.

Table 2. Experimental levels and factors.

Levels	X_1 The Right Wall of the Fertilizer Discharge Trench (°)	X_2 The Depth of the Fertilizer Discharge Trench (mm)	X_3 The Working Length of the Fertilizer Discharge Trench (mm)
−1	35	9	30
0	38	11	37
1	41	13	44

Table 3. Experimental design and results.

Serial Number	The Right Wall of the Fertilizer Discharge Trench/°	The Depth of the Fertilizer Discharge Trench/mm	The Working Length of the Fertilizer Discharge Trench/mm	Coefficient of Variation of Fertilizer Application Amount per Hole/%	Average Length of Fertilizer Application Holes/mm
	X_1	X_2	X_3	Y_1	Y_2
1	38	11	37	2.47	90.2
2	35	11	44	4.12	96.6
3	35	9	37	3.28	82.8
4	38	9	44	4.18	95.8
5	41	9	37	3.72	91
6	41	13	37	4.12	98.6
7	38	9	30	3.22	86.8
8	41	11	44	4.47	105.6
9	35	11	30	3.28	77.6
10	38	11	37	2.52	91
11	38	11	37	2.4	92.3
12	35	13	37	3.6	90.6
13	38	11	37	2.32	89.5
14	38	13	30	3.85	84
15	38	11	37	2.37	90.6
16	41	11	30	3.62	85.2
17	38	13	44	4.7	114.4

Using Design-Expert 13 software [29], the experimental data shown in Table 3 were subjected to quadratic polynomial regression analysis and variance analysis. Regression models were established for the coefficient of variation of the fertilizer application rate per hole (Y_1) and the average length of fertilizer application holes (Y_2) in relation to the three independent variables: the inclination angle of the fertilizer discharge wall (X_1), the depth of the fertilizer discharge (X_2), and the working length of the fertilizer discharge (X_3). The model equations are presented as Equation (10).

$$\begin{cases} Y_1 = 2.42 + 0.2063X_1 + 0.2338X_2 + 0.4375X_3 \\ +0.02X_1X_2 + 0.0025X_1X_3 - 0.0275X_2X_3 \\ +0.5745X_1^2 + 0.6895X_2^2 + 0.882X_3^2 \\ Y_2 = 90.72 + 4.1X_1 + 3.9X_2 + 9.85X_3 \\ -0.05X_1X_2 + 0.35X_1X_3 + 5.35X_2X_3 \\ -1.99X_1^2 + 2.02X_2^2 + 2.52X_3^2 \end{cases} \quad (10)$$

The variance analysis of the experimental results is shown in Table 4. According to Table 4, the models for the coefficient of variation of fertilizer application rate per hole (Y_1) and the average hole length (Y_2) have ($p < 0.001$), indicating that the regression models are highly significant. Additionally, the lack of fit for both models have ($p > 0.05$), which suggests that the regression models have a high goodness of fit [30].

Table 4. Analysis of variance.

Experimental Indicators	Source	Sum of Squares	df	Mean Square	F-Value	*p*-Value	Significance
Y_1	Model	9.73	9	1.08	127.53	<0.0001	**
	X_1	0.3403	1	0.3403	40.14	0.0004	**
	X_2	0.4371	1	0.4371	51.56	0.0002	**
	X_3	1.53	1	1.53	180.62	<0.0001	**
	X_1X_2	0.0016	1	0.0016	0.1887	0.6771	
	X_1X_3	0.0000	1	0.0000	0.0029	0.9582	
	X_2X_3	0.0030	1	0.0030	0.3568	0.5691	
	X_1^2	1.39	1	1.39	163.92	<0.0001	**
	X_2^2	2.00	1	2.00	236.11	<0.0001	**
	X_3^2	3.28	1	3.28	386.36	<0.0001	**
	Residual	0.0593	7	0.0085			
	Lack of Fit	0.0340	3	0.0113	1.79	0.2880	
	Pure Error	0.0253	4	0.0063			
	Cor Total	9.79	16				
Y_2	Model	1206.16	9	134.02	213.79	<0.0001	**
	X_1	134.48	1	134.48	214.53	<0.0001	**
	X_2	121.68	1	121.68	194.11	<0.0001	**
	X_3	776.18	1	776.18	1238.21	<0.0001	**
	X_1X_2	0.0100	1	0.0100	0.0160	0.9030	
	X_1X_3	0.4900	1	0.4900	0.7817	0.4060	
	X_2X_3	114.49	1	114.49	182.64	<0.0001	**
	X_1^2	16.59	1	16.59	26.47	0.0013	**
	X_2^2	17.10	1	17.10	27.27	0.0012	**
	X_3^2	26.63	1	26.63	42.49	0.0003	**
	Residual	4.39	7	0.6269			
	Lack of Fit	0.0400	3	0.0133	0.0123	0.9978	
	Pure Error	4.35	4	1.09			
	Cor Total	1210.54	16				

Note: ** indicates a highly significant difference at the 0.05 level ($p < 0.01$).

The factors affecting the coefficient of variation of the fertilizer application rate per hole (Y_1) and the influence of interactions among these factors, in descending order, are as follows: X_3^2, X_2^2, X_3, X_1^2, X_2, X_1, X_2X_3, X_1X_2, and X_1X_3. Among them, X_1, X_2, X_3, X_1^2, X_2^2, and X_3^2 have a highly significant influence on the model ($p < 0.01$), while the others are not significant.

The factors affecting the average hole length (Y_2) and the effects of interactions among these factors, from greatest to least, are as follows: X_3, X_1, X_2, X_2X_3, X_3^2, X_2^2, X_1^2, X_1X_3, and X_1X_2. Among these factors, X_1, X_2, X_3, X_2X_3, X_1^2, X_2^2, and X_3^2 have a highly significant influence on the model ($p < 0.01$), while the others are not significant. This is because the depth of the fertilizer discharge (X_2) and the working length of the fertilizer discharge (X_3) have a more significant impact on the volume of fertilizer, directly affecting the flow state of the fertilizer during the discharge process and the efficiency of discharge. Therefore, the interaction between these two factors has a more pronounced effect on the speed of fertilizer discharge.

To ensure the optimal structural parameters of the fertilizer application wheel, constraints were applied to the right wall angle, depth, and working length of the fertilizer application channel [30]. The constraint intervals are as shown in Equation (11).

$$\begin{cases} \min Y_1\{X_1, X_2, X_3\} \\ \min Y_2\{X_1, X_2, X_3\} \\ 35 \le X_1 \le 41 \\ 9 \le X_2 \le 13 \\ 30 \le X_3 \le 44 \end{cases} \tag{11}$$

Based on the constraint intervals, the results of the multi-factor experiment were optimized using Design-Expert 13. The best fertilizer application effect was achieved when the right wall angle of the fertilizer application slot was 35.16°, the depth was 10.7 mm, and the working length was 30 mm. At these parameters, the variation coefficient of the hole fertilizer application amount and the average hole length were 2.06% and 81.72 mm, respectively. Furthermore, under this parameter combination, a simulation verification test was conducted, yielding a variation coefficient of the hole fertilizer application amount and an average hole length of 1.82% and 83.6 mm, which were basically consistent with the optimization results.

4. Bench Test Platform

4.1. Test Conditions

To validate the rationality of the simulation test, a performance bench test of the fertilizer application device was conducted at different forward speeds. The optimal structural parameters for the fertilizer application wheel were 3D printed using PLA material [31]. The fertilizer application wheel was intermittently driven by a stepper motor, with an effective working length of 30 mm, corresponding to a fertilizer application amount of 4.2 g per hole. The experiments were carried out in an indoor soil tank laboratory, and the testing setup is illustrated in Figure 14. The width of the movable soil trough was 88.2 cm, and the movable length was 400 cm.

The fertilizer application device was installed on the test bench and adjusted to a reasonable height. A layer of soil was laid on the mobile soil tank to prevent the fertilizer particles from bouncing upon impact. Granular urea fertilizer was selected as the test subject. The speed of the moving soil tank was set to range from 0.4 to 1.2 m/s. Other testing equipment included a vernier caliper, a ruler, and an electronic scale with a precision of 0.001 g.

Figure 14. Bench test device. 1. Control box. 2. Fixed bracket. 3. Fertilizer tank. 4. Fertilizer distribution system. 5. Stepper motor. 6. Portable soil trench.

4.2. Testing Indicators and Measurement Methods

The selection of experimental indicators is based on GB/T 20346.2-2022 'Fertilization Machinery Part 2: Inter-row Fertilizers' production testing methods, to evaluate the fertilization performance of the fertilization device. The test used several parameters as indicators, including the coefficient of variation of fertilizer application rate per hole, the error in fertilizer application rate per hole, the average length of fertilizer application holes, and the coefficient of variation of hole length stability. The methods for determining the coefficient of variation of the fertilizer application rate per hole and the error in fertilizer application rate per hole were performed through static measurements, as illustrated in Figure 15.

Figure 15. Static measurement methods.

Due to the fertilizer particles falling onto the soil and adhering to it, it is impossible to directly weigh the amount of fertilizer particles for each hole. Therefore, when the soil trough is stationary, a stepper motor controls the intermittent rotation of the fertilizer distribution wheel at a single trough angle. A collection box is set up below the fertilizer outlet of the distribution device to measure the fertilizer amount for each hole, which is used to calculate the variation coefficient and error of the hole fertilizer application amount. The calculation formula for the coefficient of variation of the fertilizer application rate per hole is the same as that used in the simulation experiments, as shown in Equation 9. The calculation formula for the error in fertilizer application rate per is as follows:

$$q = \frac{\sum_{i=1}^{n} \frac{|Q_i - Q_0|}{Q_0}}{n} \times 100\% \quad (12)$$

where q is the error in fertilizer application rate per hole,%; where Q_i is the actual fertilizer application amount per hole, g; and where Q_0 is the theoretical fertilizer application amount per hole, g.

After the soil trough starts moving, the fertilizer distribution device operates, and after the fertilizer falls to the ground, the most concentrated point of the fertilizer particles for each hole is taken as the center. The dispersed length of the majority of the fertilizer particles that fall is measured as the hole length (L_i). The measurement method is shown in Figure 16. The average hole length (L) and the variation coefficient of hole length stability (C_L) are calculated as follows:

$$\begin{cases} L = \dfrac{1}{n}\sum\limits_{i=1}^{n} L_i \\ C_L = \dfrac{\sqrt{\dfrac{1}{n}\sum\limits_{i=1}^{n}(L_i - L)^2}}{L} \times 100\% \end{cases} \tag{13}$$

where L is the average length of fertilizer application holes, mm; where n is the number of fertilizer holes; where L_i is the length of fertilizer application hole per hole, s; and where C_L is the coefficient of variation of hole length stability,%.

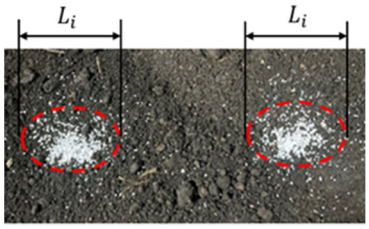

Figure 16. Fertilizer granule distribution map.

4.3. Test Results and Analysis

The condition of fertilizer particles in the 10 holes of the soil trough is statistically recorded each time, and each experimental group is repeated 5 times. The variation coefficient of the hole fertilizer application amount, the error of the hole fertilizer application amount, the average hole length, and the variation coefficient of hole length are calculated. The statistical results are shown in Table 5.

Table 5. Test results of fertilizer distribution performance at different forward speeds.

Forward Speed (m/s)	Coefficient of Variation of Fertilizer Application Rate per Hole (%)	Error in Fertilizer Application Rate per Hole(%)	Average Length of Fertilizer Application Holes (mm)	Coefficient of Variation of Hole Length Stability (%)
0.4	2.02	7.12	72.5	1.94
0.6	2.54	8.54	85.4	2.37
0.8	3.32	9.80	97.3	2.79
1.0	3.85	10.81	114.4	3.15
1.2	4.46	12.18	130.2	3.54

Table 5 shows that under the forward speed of 0.4 to 1.2 m/s, the variation coefficient of the fertilizer application amount per hole for the fertilization device ranges from 2.02% to 4.46%, the error of the fertilizer application amount per hole ranges from 7.12% to 12.18%, the average hole length is between 72.5 and 130.2 mm, and the variation coefficient of hole length stability is between 1.94% and 3.54%. All indicators meet the fertilization requirements, indicating that the working performance of the fertilization device is relatively good. Moreover, at a forward speed of 0.6 m/s, the relevant parameter indicators are

generally consistent with the simulation test results, which verifies the rationality of the simulation tests.

It is worth mentioning that the simulation tests are conducted under ideal environmental conditions, while the bench tests are affected by factors such as equipment vibrations and air resistance, which can influence the test indicators. As a result, the test data are slightly larger than that under simulation conditions; however, the overall fertilization performance meets the requirements.

5. Field Experiment

5.1. Testing Method

To verify the overall operational performance and fertilization effect of the targeted fertilization device for corn, a field experiment was conducted in June 2023 at the Sun Farm of Northeast Agricultural University in Harbin, Heilongjiang Province, as shown in Figure 17. In the experiment, small granule urea fertilizer was selected, with a fertilization depth of 110 mm and a theoretical fertilization amount of 4.2 g per corn plant. The machine's forward speed ranged from 0.4 m/s to 1.2 m/s. To facilitate the measurement of fertilizer placement performance, no soil covering was performed after the fertilization operation.

(**a**) Performance testing of fertilizer application devices.

(**b**) Effect of targeted fertilization operations.

Figure 17. Field experiment.

5.2. Test Conditions

The field experiment was conducted in accordance with the relevant testing methods and evaluation indicators specified in NY/T 1003-2006 "Technical Specification for Quality Evaluation of Fertilizing Machinery" [32]. A 10 m section of the fertilization operation was selected as a testing area to measure the variation coefficient of fertilizer distribution in the holes, the error of fertilizer distribution in the holes, the average hole length, the variation coefficient of hole length stability, and the qualification rate of fertilization position. The calculation formula for the qualification rate of fertilization position is as follows [33]:

$$\gamma = \frac{K_i}{K} \times 100\% \tag{14}$$

where K is the number of measurement points; where K_i is the number of qualified fertilization points; and where γ is the qualified rate of fertilization positions, %.

Measure the vertical distance between the corn plants and the line parallel to the furrow. Using the foot point as the center, draw a circle with a radius of 5 cm. The points where the center of the fertilizer pile fall within this circle are considered to be qualified fertilization positions. The method for calculating the qualification rate of fertilization positions involves separately counting the number of corn plants with qualified positions in each test area. The measurement method is illustrated in Figure 18.

(**a**) Determination of qualified rate of fertilization positions.

(**b**) Qualified position.

Figure 18. Qualified determination of fertilization position.

At the same speed, the data for the test indicators were calculated separately for three test areas and an average value was obtained. The field experiment data are shown in Table 6.

Table 6. Field test results.

Forward Speed (m/s)	Coefficient of Variation of Fertilizer Application Rate per Hole (%)	Error in Fertilizer Application Rate per Hole(%)	Average Length of Fertilizer Application Holes (mm)	Coefficient of Variation of Hole Length Stability (%)	Qualified Rate of Fertilization Positions (%)
0.4	2.78	7.94	81.4	2.07	84.97
0.6	3.21	9.20	91.6	2.53	89.07
0.8	3.65	10.65	106.5	2.91	94.16
1.0	3.97	11.64	123.5	3.42	91.25
1.2	4.53	12.88	141.2	3.85	86.33
Average	3.63	10.46	108.8	2.96	87.16

According to Table 6, when the machine's forward speed is between 0.4 m/s and 1.2 m/s, the coefficient of variation of the fertilizer application rate per hole, the error in fertilizer application rate per hole, the average length of fertilizer application holes, the coefficient of variation of hole length stability, and the qualification rate of fertilization position are 3.63%, 10.46%, 108.8 mm, 2.96%, and 87.16%, respectively. Due to the vibrations from the field operation, the relevant indicators are slightly higher than those from the bench test results, but the overall trend is consistent with the bench test results.

As the operation speed increases, the qualified rate of the fertilization position first increases and then decreases. This is because at lower speeds, when the fertilizer outlet has not yet reached the plant position, the system has already completed the fertilizer discharge, leading to an early fertilization position. When the forward speed is between 0.6 m/s and 1.0 m/s, the qualified rate of the fertilization position is relatively stable. However, when the forward speed reaches 1.2 m/s, the time for the fertilizer outlet to reach the plant position is slightly shorter than the system's response time, resulting in a delayed fertilization position and a relatively low qualified rate of the fertilization position. Overall, the device's performance is stable and meets the requirements for targeted deep fertilization in corn intercropping.

It is worth mentioning that this study is based on commonly used external trough wheels available on the market. However, in practical applications, factors such as the volume and friction coefficient of the fertilizer can affect fertilization performance [34]. Additionally, field tests, due to the need for a tractor towing device, exhibit more pronounced vibrations than bench tests, thereby impacting fertilization performance. In subsequent optimization designs, this issue should be considered, potentially incorporating shock

absorption and contouring mechanisms to mitigate the effects of these vibrations. Therefore, further detailed experimental research on the performance of the corn targeted deep fertilization device is needed from multiple perspectives in future work.

6. Conclusions

(1) A targeted deep fertilization device for corn has been designed, which uses a photoelectric sensor to detect the position of corn plants. A microcontroller combines the plant position information and the forward speed of the device to dynamically control the intermittent rotation of a stepping motor, thereby achieving targeted deep fertilization operations for corn.

(2) Based on cycloidal parameters, a fertilizer discharge device with a forced discharge plate mechanism was designed. Through mechanical analysis of the fertilization and discharge processes, the main factors affecting the discharge performance were identified. Coupled simulation analysis using Adams and EDEM was conducted to perform both single-factor and multi-factor experiments, examining the effects of the right wall inclination angle of the discharge, discharge depth, and discharge working length on the coefficient of variation of the hole discharge amount and the average hole length. The optimal parameter combination was determined to be a discharge wall inclination angle of 35.16°, a discharge depth of 10.7 mm, and a discharge working length of 30 mm.

(3) Bench tests and field tests were conducted. The bench tests indicated that at a forward speed of 0.4 to 1.2 m/s, under the optimal parameter combination, the coefficient of variation of the fertilizer application rate per hole of the discharge device ranged from 2.02% to 4.46%, the error in fertilizer application rate per hole ranged from 7.12% to 12.18%, the average length of fertilizer application holes ranged from 72.5 mm to 130.2 mm, and the coefficient of variation for hole length stability ranged from 1.94% to 3.54%. The field tests showed that when the machine's forward speed was between 0.4 m/s and 1.2 m/s, the coefficient of variation of the fertilizer application rate per hole, the error in fertilizer application rate per hole, the average length of fertilizer application holes, the coefficient of variation of hole length stability, and the qualification rate of fertilization position were 3.63%, 10.46%, 108.8 mm, 2.96%, and 87.16%, respectively. Overall, the device exhibited stable performance and met the requirements for targeted deep fertilization in corn cultivation.

Author Contributions: Conceptualization, Z.Q.; Data curation, Y.W.; Funding acquisition, X.S.; Investigation, Z.Z.; Project administration, Z.Q.; Software, C.L.; Validation, X.S.; Writing—original draft, Z.Q.; Writing—review and editing, C.L. All authors have read and agreed to the published version of the manuscript.

Funding: This work was supported by National Key R&D Program of China (2023YFD2301602-1), the Key Joint Project of the Natural Science Foundation of Heilongjiang Province, the Funding for the Opening Project of The National Key Laboratory of Smart Farm Technology and Systems, the Heilongjiang Provincial key research and development program (2022ZX05B05), and the Heilongjiang Natural Science Foundation research team project (TD2023E001).

Institutional Review Board Statement: Not applicable.

Data Availability Statement: The data of this study can be obtained from the corresponding authors.

Conflicts of Interest: The authors declare no conflicts of interest.

References

1. Zhao, X.G. Research status and analysis on fertilization technology of corn topdressing machinery. *J. Agric. Mech. Res.* **2021**, *43*, 1–9.
2. Tang, H.; Wang, J.; Xu, C.; Zhou, W.; Wang, J.; Wang, X. Research progress analysis on key technology of chemical fertilizer reduction and efficiency increase. *Trans. Chin. Soc. Agric. Mach.* **2019**, *50*, 4.

3. Zong, Z.; Liu, G. Design and Experiment of Maize Fertilization Control System Based on Machine Vision. *Trans. Chin. Soc. Agric. Mach.* **2021**, *52*, S1.
4. Hu, H.; Li, H.; Wang, Q.; He, J.; Zhang, Y.; Chen, W.; Wang, X. Design and experiment of targeted hole-pricking and deep-application fertilizer applicator between corn rows. *Trans. Chin. Soc. Agric. Eng.* **2016**, *32*, 26–35.
5. Li, M.T.; Wen, X.Y.; Zhou, F.J. Working parameters optimization and experiment of precision hole fertilization control mechanism for intertilled crop. *Trans. Chin. Soc. Agric. Mach.* **2016**, *47*, 37–43.
6. Wan, L.; Xie, D.; Li, Y.; Chen, L. Design and experiment of roller hole fertilizer application between corn rows. *Trans. Chin. Soc. Agric. Mach.* **2020**, *51*, 64–73.
7. Wang, Z.; Liang, C.; Wang, H. Design and experiment of corn variable hole fertilization test bed. *Mech. Res.* **2020**, *42*, 166–169.
8. Zhao, S.; Zong, Z.; Liu, G. Design and Test on Position Fertilization Control System Based on Motor Drive. *Trans. Chin. Soc. Agric. Mach.* **2019**, *50*, 91–95.
9. Zhang, S.F. *Fertilization Guidelines for Major Crops in China*; China Agriculture Press: Beijing, China, 2009; pp. 1–10.
10. Du, X.; Liu, C.; Jiang, M.; Yuan, H.; Dai, L.; Li, F. Design and experiment of inclined trapezoidal hole fertilizer point-applied discharging device. *Trans. Chin. Soc. Agric. Mach.* **2021**, *52*, 43–53.
11. Wang, J.; Zhou, W.; Wang, J.; Zhang, C.; Jiang, D. Experiment and Optimization of Working Parameters for Pricking Hole Mechanism of Oblique Type Non-circular Gears Planetary System. *Nongye Jixie Xuebao/Trans. Chin. Soc. Agric. Mach.* **2017**, *48*, 66–70.
12. Zhu, Q.; Wu, G.; Chen, L.; Zhao, C.; Meng, Z. Influences of structure parameters of straight flute wheel on fertilizing performance of fertilizer apparatus. *Trans. CSAE* **2018**, *34*, 12–20.
13. Liao, Q.; Chen, Y.; Zhang, Q.; Wang, L.; Lin, J.; Du, W. Design and Experiment of Side Deep Hole Fertilization Device for Rapeseed. *Trans. Chin. Soc. Agric. Mach.* **2023**, *54*, 41–52.
14. Dun, G.; Yu, C.; Guo, Y.; Ji, W.; Islam, K.R.; Du, J. Design and experiment of double-gear type fertilizer apparatus. *Nongye Jixie Xuebao/Trans. Chin. Soc. Agric. Mach.* **2020**, *51*, 87–96.
15. Liu, C.; Wei, D.; Du, X.; Jiang, M.; Song, M.; Zhang, F. Design and test of wide seedling strip wheat precision hook-hole type seed-metering device. *Nongye Jixie Xuebao/Trans. Chin. Soc. Agric. Mach.* **2019**, *50*, 53–62.
16. Liu, J.; Zhu, D.; Tai, Q.; Yu, C.; Wang, T.; Xue, K.; Zhang, S.; Liao, J. Design and experiment of adjustable socket-wheel precision fertilizer apparatus for dry direct-seeding rice. *INMATEH-Agric. Eng.* **2021**, *63*, 121–130.
17. Wang, J.; Fu, Z.; Weng, W.; Wang, Z.; Wang, J.; Yang, D. Design and Experiment of Conical-disc Push Plate Double-row Fertilizer Apparatus for Side-deep Fertilization in Paddy Field. *Trans. Chin. Soc. Agric. Mach.* **2023**, *54*, 53–62.
18. Zhang, J.; Liu, H.; Gao, J.; Lin, Z.; Chen, Y. Simulation and test of corn layer alignment position hole fertilization seeder based on SPH. *Trans. Chin. Soc. Agric. Mach.* **2018**, *49*, 66–72.
19. Yuan, W.; Li, K.; Jin, C.; Hu, M.; Zhang, W. Design and experiment of hill placement fertilizer applicator. *J. Agric. Mech. Res.* **2018**, *40*, 145–149+165.
20. Liu, Z.; Wang, Q.; Liu, C.; Li, H.; He, J.; Liu, J. Design and experiment of precision hole-fertilizing apparatus with notched plate. *Trans. Chin. Soc. Agric. Mach.* **2018**, *49*, 137–144.
21. Wu, N.; Lin, J.; Li, B. Design and Test on No-tillage Planter Precise Hole Fertilization System. *Trans. Chin. Soc. Agric. Mach.* **2018**, *49*, 64–72.
22. Zhu, H.; Wu, X.; Bai, L.; Qian, C.; Zhao, H.; Li, H. Development of the biaxial stubble breaking no-tillage device for rice stubble field based on EDEM-ADAMS simulation. *Trans. Chin. Soc. Agric. Eng.* **2022**, *38*, 10–22.
23. Guo, Y.; Liu, J.; Yin, H.-L.; Zhang, Q.; Li, L.-T.; Wang, Y.-L. Effects of quantitative fertilization by a single plant on the yield, nutrient absorption, and utilization of summer maize. *J. Agric. Resour. Environ.* **2020**, *37*, 924–930.
24. Pan, R.; Meng, Z.; Dong, J.; Shang, Y.; Mei, H.; Yan, B.; Gu, W.; Gao, N.; Xue, Z.; Zhang, Z. Design and testing of an intermittent fertilisation method for seeding of maize (*Zea mays*). *Crop Pasture Sci.* **2022**, *73*, 203–213. [CrossRef]
25. Wu, R.; Zhang, L.; Qian, F.; Cai, H. Design and simulation of cave-fertilizer apparatus for maize. *J. Anhui Agric. Univ.* **2017**, *44*, 941–946.
26. Yuan, Q.; Xu, L.; Xing, J.; Duan, Z.; Ma, S.; Yu, C.; Chen, C. Parameter calibration of discrete element model of organic fertilizer particles for mechanical fertilization. *Trans. CSAE* **2018**, *34*, 21–27.
27. Zhou, W.; An, T.; Wang, J.; Fu, Q.; Wen, N.; Sun, X.; Wang, Q.; Liu, Z. Design and experiment of a targeted variable fertilization control system for deep application of liquid fertilizer. *Agronomy* **2023**, *13*, 1687. [CrossRef]
28. Liang, Y.; Tang, Z.; Ji, C.; Zheng, X.; Liu, J.; Li, Q.; Zhang, L. Optimization and Experiment of Structural Parameters of Outer Groove Wheel Fertilizer Drainer. *J. Agric. Mech. Res.* **2023**, *45*, 7–14.
29. Song, C.; Zhou, Z.; Wang, G.; Wang, X.; Zang, Y. Optimization of the groove wheel structural parameters of UAV-based fertilizer apparatus. *Transact. Chin. Soc. Agric. Eng.* **2021**, *37*, 1–10.
30. Ding, S.; Bai, L.; Yao, Y.; Yue, B.; Fu, Z.; Zheng, Z.; Huang, Y. Discrete element modelling (DEM) of fertilizer dual-banding with adjustable rates, Comput. *Electron. Agric.* **2018**, *152*, 32–39. [CrossRef]
31. Du, X.; Liu, C.; Jiang, M.; Yuan, H.; Dai, L.; Li, F. Calibration of bonding model parameters for coated fertilizers based on discrete element method. *Trans. Chin. Soc. Agri. Mach.* **2022**, *53*, 141–149.
32. Yang, X.; Wang, J.; Yang, J.; Zhao, L.; Li, Q. Design and test of stacking type fertilizer discharge adjusting device for ditching fertilizer applicator. *J. Chin. Agric. Mech.* **2023**, *44*, 26–34.

33. Du, J.; Yang, Q.; Xia, J.; Li, G. Discrete element modeling and verification of an outer groove wheel fertilizer applicator with helical teeth. *Trans. ASABE* **2020**, *63*, 659–665. [CrossRef]
34. Lei, X.; Yang, W.; Liu, L.; Liu, H.; Ren, W.; Chen, Y. Design and experiment of seed hill feeding device in pneumatic centralized metering device for hybrid rice. *Trans. CSAM* **2018**, *49*, 58–67.